www.czasopisma.pan.pl PAN POLSKA AKADEMIA NAUK www.journals.pan.pl

PAN ARCHIVES OF ACOUSTICS
Vol. **39**, No. 1, pp. 139–144 (2014)

DOI: 10.2478/aoa-2014-0014

Noninvasive Imaging of Thermal Fields Induced in Soft Tissues In Vitro by Pulsed Focused Ultrasound Using Analysis of Echoes Displacement

Piotr KARWAT, Jerzy LITNIEWSKI, Tamara KUJAWSKA, Wojciech SECOMSKI, Kazimierz KRAWCZYK

Institute of Fundamental Technological Research
Polish Academy of Sciences
Pawińskiego 5B, 02-106 Warszawa, Poland; e-mail: pkarwat@ippt.pan.pl

(*received July 9, 2013; accepted February 28, 2014*)

Therapeutic and surgical applications of focused ultrasound require monitoring of local temperature rises induced inside tissues. From an economic and practical point of view ultrasonic imaging techniques seem to be the most suitable for the temperature control. This paper presents an implementation of the ultrasonic echoes displacement estimation technique for monitoring of local temperature rise in tissue during its heating by focused ultrasound The results of the estimation were compared to the temperature measured with thermocouple. The obtained results enable to evaluate the temperature fields induced in tissues by pulsed focused ultrasonic beams using non-invasive imaging ultrasound technique.

Keywords: HIFU, therapeutic ultrasound, ultrasonic imaging, echo strain estimation.

1. Introduction

In modern medicine the ultrasound (US) has many applications such as ultrasonic imaging of selected organs, their therapy and surgery (Haar, 2007). In diagnostic applications the exposure to ultrasound is at a level safe for patient but still sufficient to get an acceptable signal-to-noise ratio (SNR). An aim of a diagnostic ultrasound is to obtain the required information without causing adverse cellular effects. In contrast, therapeutic or surgical applications require that sonicated tissue lesions were subjected to reversible or irreversible thermal changes depending on a target of the treatment. Therapeutic ultrasound energy is usually delivered as pulsed waves focused in a localized tumor. A main goal of many therapeutic applications of ultrasound is tissue heating. An efficiency of such therapies depends on a precision of localization and amplitude of the induced temperature rise. Currently the most popular method of imaging of local thermal fields induced in tissues by therapeutic ultrasonic beams is Magnetic Resonance Imaging (MRI). The MRI-guided High Intensity Focused Ultrasound (HIFU) enables new therapeutic applications (Hynynen, 2010).

The main disadvantage of the combination of these two modalities is high cost of the MRI technique which limits its applications. Our objective was to develop an alternative method based on diagnostic US modality for temperature control inside tissues heated locally by focused ultrasonic beams. There are several methods for non-invasive estimation of temperature rise induced in tissue by focused US. One can take advantage of the instantaneous changes in frequency as proposed in (Liu, 2009). Another method described in publication (Guiot, 2004) is based on an analysis of the average grey-scale level of the classical B-mode image. Thermal changes also influence the acoustic wave propagation velocity, which is used in the Echo Strain Estimation (ESE) algorithm proposed in (Miller, 2002). In our work the ESE method was applied for estimation of the temperature rise induced in beef liver in vitro by pulsed focused ultrasonic beam of 2.1 W acoustic power.

2. Materials and methods

All measurements were carried out at 36°C. The setup for invasive measurements is shown in Fig. 1.

The acoustic pressure tone bursts were generated at the surface of the PZT (Pz26, Meggitt, Denmark) circular focused transducer with a 2 MHz resonance

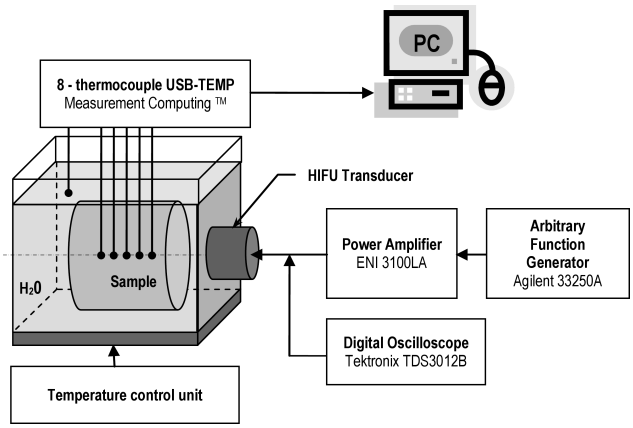

Fig. 1. Block-scheme of the experimental setup for invasive temperature measurements.

frequency, 15 mm diameter and 25 mm radius of curvature. The transducer was air-backed, had a quarter wavelength matching layer and was driven at its resonance frequency by 20-cycle tone bursts with a duty-cycle of 0.2. The transmission electronics were based on an arbitrary function generator (Agilent 33250A, Colorado Springs, USA) that defined both the frequency and pulsing mode of tone bursts generated. Then the signal was amplified with a power amplifier (55 dB gain, ENI 3100LA, Rochester, NY, USA). The tone burst waveform was displayed with a digital oscilloscope (Tektronix TDS3012B, Beaverton, USA). The output of the amplifier excited the PZT transducer to produce the ultrasonic field. The transducer was mounted in a water tank with controlled temperature. The source pressure was determined by two methods. First, using the calibrated needle hydrophone S/N 1661 (Precision Acoustics, Dorchester, UK) with the active element diameter of 0.2 mm and next, using the Ultrasound Power Meter (Ohmic Instruments UPM-DT1E, Easton, USA). The source pressure used was found to be 0.37 MPa (average acoustic power of the beam was equal 2.1 W).

All tissue samples being tested were obtained from a slaughterhouse. Experiments were done within 8 hours after slaughter. Each sample was degassed and inserted in a cylindrical chamber (of 30 mm diameter and 20 mm height). The chamber had a 20-μm thick, transparent for sound, polyethylene foil stretched over each end and was placed in the water tank. The distance between the transducer and the water-tissue interface was selected in such way as to maximize nonlinear effects (generation of harmonics) induced in tissues by the HIFU. It was chosen on the basis of the numerical simulation of the nonlinear propagation of the generated tone burst in water. The water-tissue interface was set at the position where the amplitude of the second harmonic component begins to grow rapidly. For the transducer used this distance was found to be 15 mm. In previous publications (Kujawska, 2011; 2012) it was shown that for circular sources with $ka \gg 1$ (here k is the wave number, a denotes transducer radius), generating weak or moderate nonlinear fields in water, the distance at which a sudden growth of the second harmonic amplitude begins is constant regardless of the source pressure.

The temperature rise induced in tissues by the HIFU was measured by five thermocouples with a diameter of 0.2 mm. They were inserted in the tissue sample using thin, 0.5 mm in diameter hypodermic needles fixed to the tank cover in order to ensure their precise position on the acoustic beam axis in steps of 5 mm. The uncertainty of the thermocouple tip positions was ± 0.2 mm. Due to small diameter of the thermocouples their influence on measurement results were negligible. The temperature rise detected by each thermocouple was recorded with 1 second step by the USB-TEMP unit (Measurement Computing, Norton, USA) and transferred to the PC memory. For processing of the data obtained and visualization of the curves of the temperature rise *versus* time $\Delta T(t)$ the software TracerDAQ was used. The maximum temperature rise determined the position of the focal spot.

The temperature rise induced in the tested tissue sample by the HIFU beam and measured at its focal spot is shown in Fig. 2.

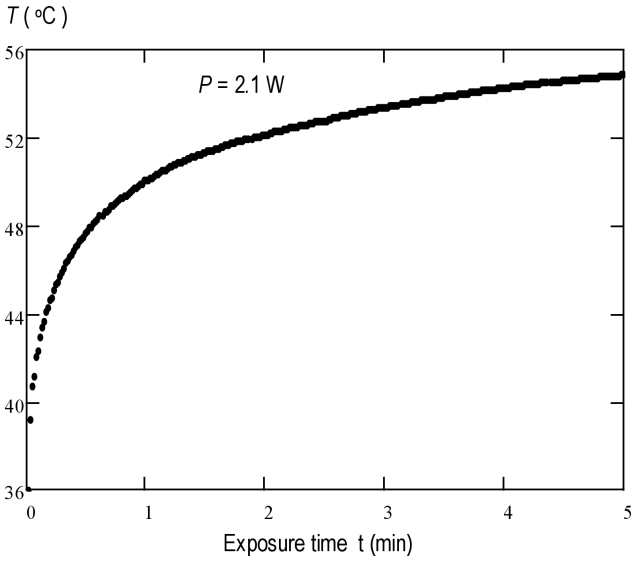

Fig. 2. Temperature rise induced in a beef liver *in vitro* by the pulsed focused ultrasonic beam of 2.1 W average acoustic power and measured by thermocouple inserted in the beam focal spot during 5 min exposure.

In order to measure the temperature rise non-invasively the setup was modified as shown in Fig. 3. The ultrasonic imaging system Sonix TOUCH (Ultrasonix, British Columbia, Canada) with a linear probe L14-5/38 operating at the 10 MHz frequency

was used for raw data collection. The system has an access to radio-frequency (RF) echo signals. The RF echoes were recorded from each scan-line in the focal plane of the HIFU beam. The signal processing was done with use of the Matlab software (Mathworks Inc., Natick, Massachusets, USA). A conversion of the recorded RF waveforms to the temperature map was done through the ESE method. This technique is based on the relationship between the sound velocity in tissues and their temperature. Figure 4 shows a principle of this method. As the tissue is being locally heated by the HIFU, its acoustic properties are changing. As a result the return time delay of ultrasonic echoes from structures beneath is also modified. The comparison of signals recorded before and after temperature change allows to calculate the echoes displacement and thus to estimate a local change of the sound velocity in tissues and to evaluate their temperature rise.

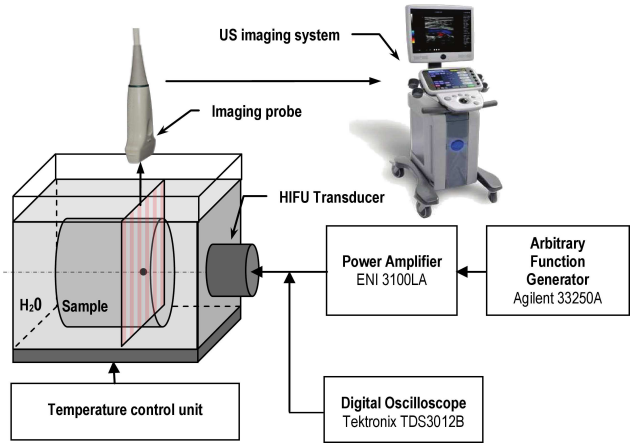

Fig. 3. Block-scheme of the experimental setup for non-invasive temperature measurements.

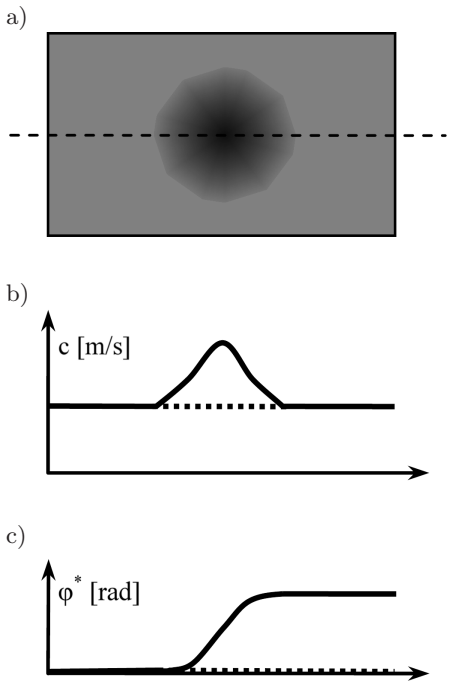

Fig. 4. Illustration of the principle of the ESE method: a) a distribution of the sound velocity in the sample with the HIFU focal spot in its center and a selected scan-line drawn through the heated area, b) a sound velocity and c) a phase shift of the signal along the selected scan-line.

The formula for the relative change in the sound velocity can be deduced from the general formula for the signal phase φ:

$$\varphi = 2zk = 2\pi F_n \frac{2z}{c}, \tag{1}$$

where z denotes the depth and k is the wave number for the nominal frequency F_n and the sound velocity c. Let us define phases $\varphi_{1\,\mathrm{init}}$ and $\varphi_{2\,\mathrm{init}}$ which are related to two axially adjacent sampling points (pixels) and can be detected at the initial state before the heating:

$$\varphi_{1\,\mathrm{init}} = 2\pi F_n \frac{2z}{c_0}, \tag{2}$$

$$\varphi_{2\,\mathrm{init}} = 2\pi F_n \frac{2(z+\Delta z)}{c_0}. \tag{3}$$

The Δz is the distance between the neighboring pixels while c_0 stands for the sound velocity before any thermal modification. When the heating is applied the sound velocity changes by Δc and the formulas (2) and (3) are modified as follows:

$$\varphi_1 = 2\pi F_n \frac{2z}{c_0 + \Delta c}, \tag{4}$$

$$\varphi_2 = 2\pi F_n \frac{2(z+\Delta z)}{c_0 + \Delta c}. \tag{5}$$

Next, let φ_1^* and φ_2^* represent the phase shifts at the considered pixel locations:

$$\varphi_1^* = \varphi_1 - \varphi_{1\,\mathrm{init}} = 2\pi F_n 2z \left(\frac{1}{c_0+\Delta c} - \frac{1}{c_0}\right), \tag{6}$$

$$\varphi_2^* = \varphi_2 - \varphi_{2\,\mathrm{init}} = 2\pi F_n 2(z+\Delta z)\left(\frac{1}{c_0+\Delta c} - \frac{1}{c_0}\right). \tag{7}$$

The difference between the phase shifts $\Delta\varphi$ is then equal:

$$\Delta\varphi = \varphi_2^* - \varphi_1^* = 2\pi F_n 2\Delta z \left(\frac{-\Delta c}{(c_0+\Delta c)c_0}\right). \tag{8}$$

As the Δc is small in comparison to c_0, the following simplification is used:

$$c_0 + \Delta c \cong c_0. \tag{9}$$

Equation (8) can be rewritten as follows:

$$\Delta\varphi = 2\Delta z k_0 \frac{-\Delta c}{c_0}, \tag{10}$$

where k_0 denotes the wave number:

$$k_0 = 2\pi F_n / c_0. \tag{11}$$

The final formula for the relative changes in the sound velocity is obtained through rearrangement of the Eq. (10):

$$\frac{\Delta c}{c_0} = \frac{-\Delta\varphi}{2\Delta z k_0}. \tag{12}$$

This formula is a simplified form of the equation derived in (Souchon, 2005) which is based on shifts in echo return time delay instead of the phase shifts and, moreover, takes into account a thermal strain of the sample structure. In fact, the mechanical deformations result in phase shifts which are indistinguishable from those produced by the sound velocity changes. The final results therefore contain the inseparable information on both: the sound velocity change and the mechanical strain.

The presented algorithm is based on the Eq. (12). The k_0 and Δz are known while the $\Delta\varphi$ can be derived from the received RF waveforms. A block diagram of the procedure for temperature change estimation is shown in Fig. 5.

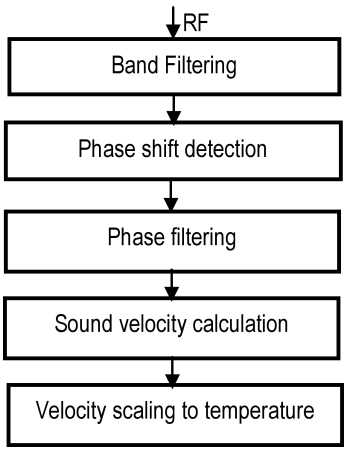

Fig. 5. Block-scheme of the algorithm used for estimation of temperature fields induced in tissues by HIFU using the Echo-Strain Estimation method.

First, the RF waveforms are band-pass filtered which removes the interference from the HIFU and reduces noise. Then, the signal phase φ is derived from the complex data obtained through the Hilbert transform. Next, the algorithm calculates the phase shifts φ^* between the RF echoes recorded before the heating and at a selected moment during the heating.

$$\varphi^*(x,z,n) = \varphi_{uw}(x,z,n) - \varphi(x,z,n_0). \tag{13}$$

The φ_{uw} is the phase φ unwrapped along the corresponding pixels of the successive recorded image frames, the x and z are the coordinates of each image pixel in the lateral and axial directions, respectively, the n is the number of the image frame and the n_0 denotes the first frame which is regarded as a reference for imaging of the subsequent relative changes in the sound velocity. The $\varphi^*(x,z,n)$ is proportional to the integral of the sound velocity changes along the image lines in the range from 0 to z, which is shown in Fig. 4. Therefore, in accordance with the Eq. (12), the further processing involves differentiation which, however, amplifies the noise. Thus, to achieve an acceptable level of readability, the φ^* was subjected to a low-pass filtration. Then the relative change of the sound velocity in the sample was calculated according to the following formula, being an equivalent to the Eq. (12):

$$\frac{\Delta c}{c_0} = \frac{-\left(\varphi^*(x,z+\Delta z,n) - \varphi^*(x,z,n)\right)}{2\Delta z k}. \tag{14}$$

Knowing the distribution of changes in the sound velocity the temperature field can be calculated in accordance to the temperature – sound velocity dependences such as those presented in (Bamber, 1979).

3. Results and discussion

The temperature rise measured with a thermocouple located in the focal spot of the HIFU beam is shown in Fig. 2. The obtained results allowed to assess the heating process in tested tissues and were regarded as a reference for temperature field estimated by the non-invasive imaging technique. It is evident from Fig. 2 that an exposure of tested tissues to HIFU of 2.1 W average acoustic power may lead to the local temperature rise to about 54°C during 5 minutes. However, this time was not sufficient to observe any changes of the tissue structure in the B-mode images (see Fig. 6). Only the results of the RF data processing by means of the described algorithm clearly show changes in the temperature distribution compared with the situation before the heating (see Fig. 7).

It should be noted that the relationship between the sound velocity and the temperature varies between patients depending on their individual characteristics e.g. state of health (Bamber, 1981). Thus, at the present stage of investigations the scaling of the results to the values expressed in Celsius degrees is only approximate, accomplished on the base of the invasive measurements carried out with use of the thermocouple.

In the reconstructed temperature map a shadow artifact appeared below the heated spot. In the future work an attempt to remove the reasons of its formation and to improve the presented algorithm will be undertaken.

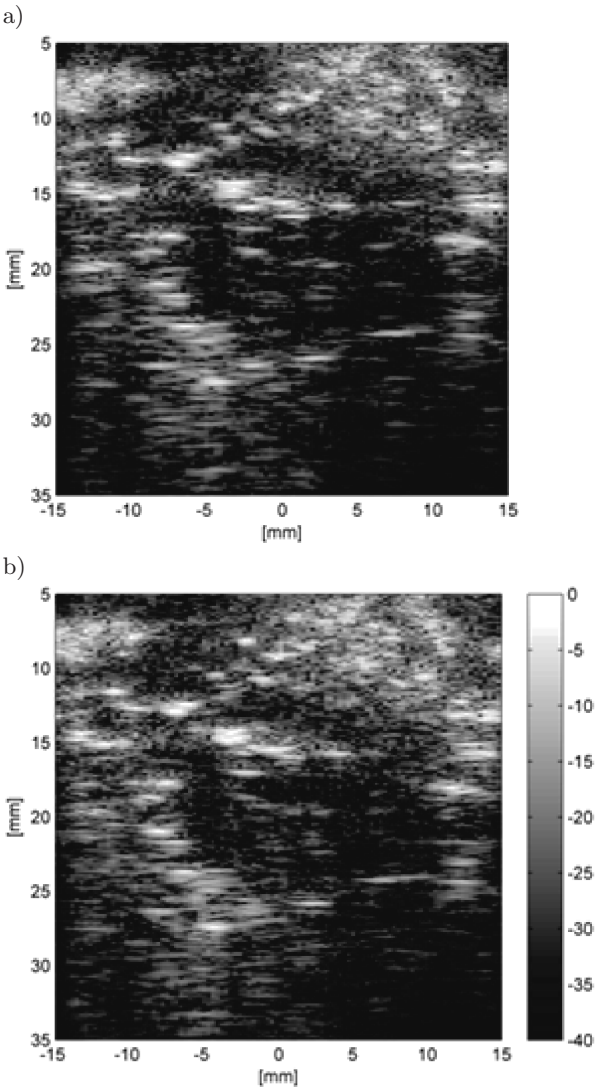

Fig. 6. Ultrasonic B-mode images of the heated tissue area: a) before and b) after 5 min exposure to HIFU.

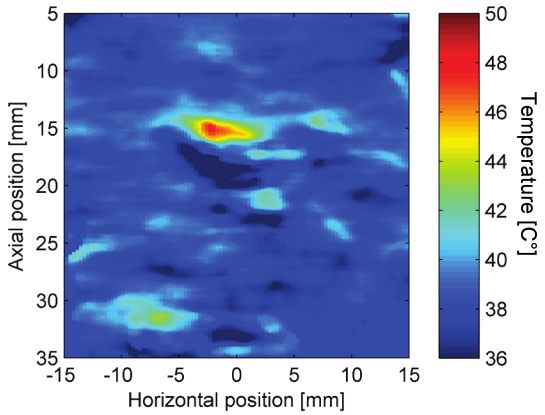

Fig. 7. Map of the temperature distribution in the HIFU focal plane.

Apart from the signal originating from the sound velocity change, the temperature map also contains areas with probably false signal that can be related to insufficient SNR which, in turn, could lead to local accumulation of errors resulting from noise. In order to provide a proper temperature imaging conditions it is necessary to ensure that the SNR is at a sufficient level. The issue of the SNR required for proper temperature imaging with use of the presented method should be examined more closely. This problem for a similar algorithm was described in more detail in (Miller, 2002).

Moreover, the artifacts can be caused by mechanical deformations resulting from thermally induced stresses and also by tissue denaturation that usually occurs at temperatures higher than 44°C. Both effects are a source of distortions in the temperature map obtained with use of the ESE technique. These artifacts can be of comparable or even higher amplitude than the useful part of the temperature map. Therefore, it is recommended to reduce the possibility of their occurrence at the stage of measurement design.

The presented results are preliminary data for studying the non-invasive ultrasonic measurements of temperature rises induced in tissues by the HIFU. The presented algorithm is a promising tool to realize the non-invasive monitoring of the temperature fields during treatment based on the thermal effects.

Acknowledgments

The financial support of the Ministry of Science and Higher Education of Poland and the National Science Centre (Projects 2011/01/B/ST7/06728; 2011/01/B/ST7/06735) is gratefully acknowledged.

References

1. Bamber J.C., Hill C.R. (1979), *Ultrasonic attenuation and propagation speed in mammalian tissues as a function of temperature*, Ultrasound. Med. Biol., **5**, 149–157.
2. Bamber J.C., Hill C.R., King J.A. (1981), *Acoustic properties of normal and cancerous human liver – II Dependence on tissue structure*, Ultrasound Med. Biol., **7**, 135–144.
3. Guiot C., Cavalli R., Gaglioti P., Danelon D., Musacchio C., Trotta M., Todros T. (2004), *Temperature monitoring using ultrasound contrast agents: in vitro investigation on thermal stability*, Ultrasonics, **42**, 927–930.
4. Haar G. ter (2007), *Therapeutic applications of ultrasound*, Progress in Biophysics and Molecular Biology, **93**, 11–129.
5. Hynynen K. (2010), *MRI-guided focused ultrasound treatments*, Ultrasonics, **50**, 221–229.
6. Kujawska T., Nowicki A., Lewin P.A. (2011), *Determination of nonlinear medium parameter B/A using model assisted variable-length measurement approach*, Ultrasonics, **51**, 997–1005.

7. Kujawska T. (2012), *Pulsed focused nonlinear acoustic fields from clinically relevant therapeutic sources in layered media: experimental data and numerical prediction results*, Archives of Acoustics, **37**, 3, 269–278.

8. Liu H.-L., Li M.-L., Shih T.-C., Huang S.-M., Lu I.-Y., Lin D.-Y., Lin S.-M., Ju K.-C. (2009), *Instantaneous frequency-based ultrasonic temperature estimation during focused ultrasound thermal therapy*, Ultrasound in Med. & Biol., **35**, 10, 1647–1661.

9. Miller N.R., Bamber J.C., Meaney P.M. (2002), *Fundamental limitations of noninvasive temperature imaging by means of ultrasounds echo strain estimation*, Ultrasound in Med. & Biol., **28**, 10, 1319–1333.

10. Souchon R., Bouchoux G., Maciejko E., Lafon C., Cathignol D., Bertrand M., Chapelon J.-Y. (2005), *Monitoring the formation of thermal lesions with heat-induced echo-strain imaging: a feasibility study*, Ultrasound in Med. & Biol., **31**, 2, 251–259.